Retrosplenial segregation reflects the navigation load during ambulatory movement

Tien-Thong Nguyen Do, Tzyy-Ping Jung, *Fellow, IEEE*, Chin-Teng Lin, *Fellow, IEEE*

***Abstract*—Spatial navigation is a complex cognitive process based on vestibular, proprioceptive, and visual cues that are integrated and processed by an extensive network of brain areas. The retrosplenial complex (RSC) is an integral part of coordination and translation between spatial reference frames. Previous studies have demonstrated that the RSC is active during a spatial navigation tasks. The specifics of RSC activity under various navigation loads, however, are still not characterized. This study investigated the local information processed by the RSC under various navigation load conditions manipulated by the number of turns in the physical navigation setup. The results showed that the local information processed via the RSC, which was reflected by the segregation network, was higher when the number of turns increased, suggesting that RSC activity is associated with the navigation task load. The present findings shed light on how the brain processes spatial information in a physical navigation task.**

***Index Terms*—EEG, spatial navigation, mental workload, MoBI**

I. Introduction

SPATIAL navigation is an essential human skill. Without it, we would be lost—literally. However, in comparison to other areas of the brain, relatively little is known about how the human sense of direction works. We know that several regions of the brain [1, 2] are involved in integrating and translating our movements [3], visual cues, proprioceptive information, and other sensory inputs into a mental representation of space [4]. One of these brain regions is the retrosplenial complex (RSC) [5], which is a central hub between the areas of the brain that govern visual processing, associations, learning, and memory and is indirectly linked to planning and decision-making. The RSC is thought (but not confirmed) to act as a bridge between perception and memory and may be involved in imagining future events or processing scenes. Studies have also shown that the RSC plays an important role in helping us switch between spatial reference frames [6, 7]: egocentric (self-centered) navigation, where we view the world around us in relation to ourselves, and allocentric (world-centered) navigation, where we reference one object to another [8].

However, only a few studies have explored brain dynamics in spatial navigation in full-body movement due to the limitations of brain imaging hardware. The stationary experiment involved participants laying still in a functional magnetic resonance imaging (fMRI) machine [1]; therefore, these experiments were not designed to explore the neural mechanisms that contribute to navigation in real-world environments. Other studies did involve freely moving participants, but the participants were clinical subjects suffering from severe epilepsy [9, 10].

Moreover, cognitive function depends on sufficient configuration among brain regions, reflected by distinct connectivity patterns [11]. Thus, examining brain network properties could help us better understand the underlying mechanism of cognitive function. There is clear evidence of a relationship between cognitive performance, network segregation and network integration, which are essential attributes of the brain network. Notably, a decline in network segregation leads to lower cognitive performance [12-15].

Nevertheless, many functional connectivity (FC) studies have investigated the larger-scale brain network, which may not reflect the involvement of each region in task execution. Those studies performed analyses at the global level and considered all the nodes of the brain to have the same roles, as opposed to scrutinizing specific brain regions related to the experimental task. Furthermore, brain network segregation and integration are not generalized for all tasks and rely on the cognitive demand of specific tasks [16]. For instance, at the global level, in the N-back experiment, the 2-back showed a higher integration than the 0-back [16-18]. Moreover, trial accuracy was positively related to network integration [16]. However, this feature is not the same for all subnetworks in the brain and even contradicts findings in the frontoparietal network [18].

A few studies have investigated specific brain regions related to experimental tasks. A study on sensorimotor performance demonstrated that reduced sensorimotor network segregation leads to poorer behavioral performance [14]. The same relationship between sensorimotor network segregation and performance has been found at the whole-brain level [13]. Moreover, increased network segregation reflects the greater

This work was supported in part by the Australian Research Council (ARC) under Discovery Grant DP180100670 and Discovery Grant DP180100656; in part by the Australia Defence Innovation Hub under Contract P18-650825; U.S. Office of Naval Research Global through Cooperative Agreement under Grant ONRG-NICOP-N62909-19-1-2058; and in part by the NSW Defence Innovation Network and NSW State Government of Australia under Grant DINPP2019 S1-03/09.

T.-T. N. Do, and C.-T. Lin are with the Australian Artificial Intelligence Institute, University of Technology Sydney, Ultimo, NSW, Australia (correspondence e-mail: nguyentienthong.do@uts.edu.au).

T.-P. Jung is with the Swartz Center for Computational Neuroscience, University of California at San Diego, La Jolla, CA 92093 USA.

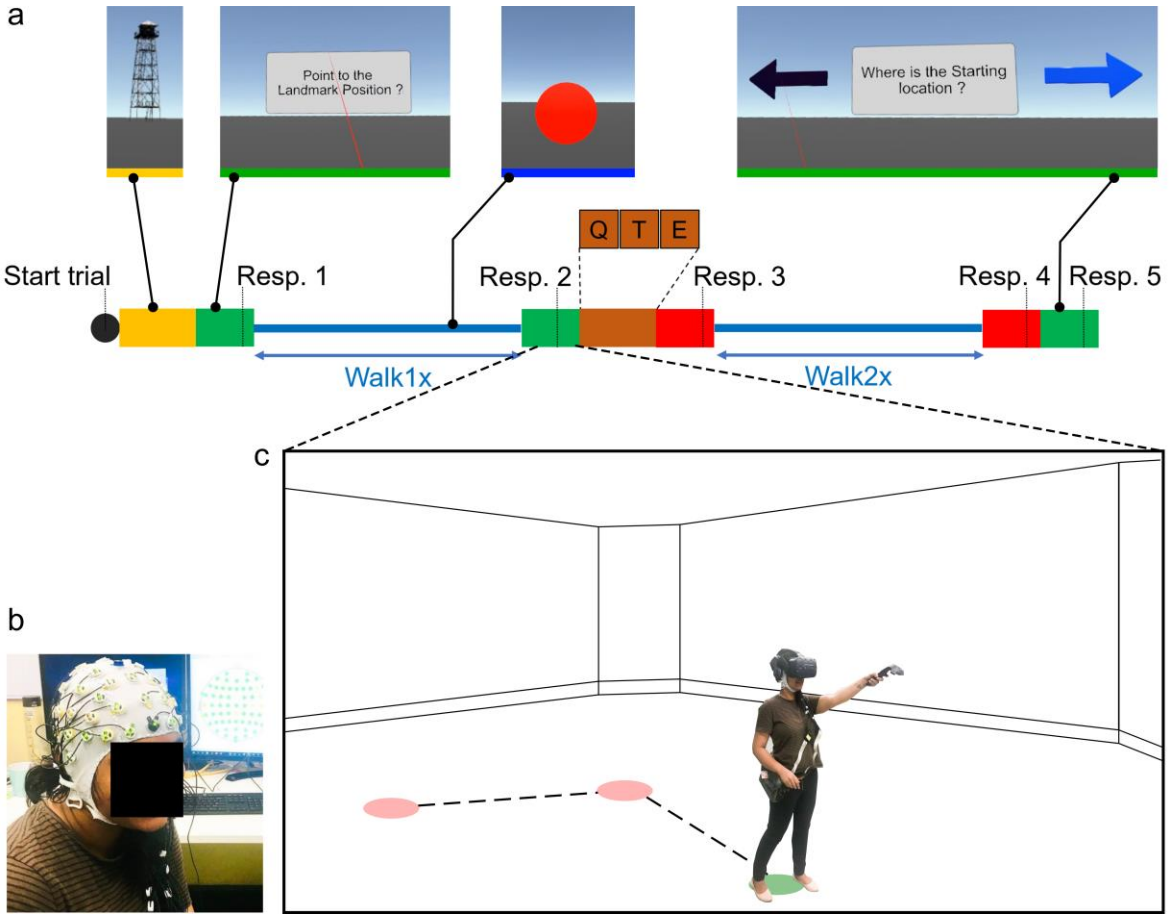

Fig. 1. The experimental design. (a) Trial representation. At the beginning of the trial, participants had 4 seconds to remember a landmark, which was presented approximately 200 meters in front of them. Then, the landmark disappeared (in the rest of the trial), and participants answered the question: "Where is the landmark position?" (Resp. 1, green square). Next, participants freely walked in a predefined path with the number of turns points being randomly chosen as 2 or 3 (walk 1x). Subsequently, participants were asked to recall the landmark position (Resp. 2, green square). Next, participants encoded a set of letters (3, 5, or 7 letters) (orange square) and then performed the letter-retrieval task (Resp. 3, red square). Then, participants started the second walk (2x) with 2 or 3 turn points. After finishing the walk, participants performed the letter-retrieval task (Resp. 4, red square) and spatial-retrieval task (Resp. 5, green square). (b) EEG cap set up. (c) The participant responded to a landmark position.

autonomy of task-related networks and saves resources for other cognitive demands [19]. Thus, there might be a mechanism to segregate brain tasks related to processing cognitive tasks.

Furthermore, investigating brain activity across a network under a specific frequency might rigorously reflect their attributions. Theta frequency has been revealed as an important mechanism of grid-cell network activity in ambulatory navigation [20-22]. In addition, theta frequency was modulated and correlated with the mental workload and was reflected in the frontal midline region [23]. Therefore, examining the network properties under a specific frequency in a distinct brain region related to an experimental task may reflect a precise mechanism of the brain network in a specific task-related brain region [24]. In short, studying a large-scale brain network may reflect the whole cognitive stage of the brain but might not fully reveal the specific mechanism of the task-related brain region. It is necessary to investigate the segregation and integration of specific brain regions related to the experimental task.

This study investigated the brain network dynamics of healthy human participants during active navigation under various workload conditions. To overcome the movement restrictions associated with standard brain imaging modalities, such as fMRI, we adapted a mobile brain/body imaging (MoBI) system [25-27] to give participants the freedom to move naturally. We equipped participants with a high-density electroencephalogram (EEG) cap synchronized to a head-mounted virtual reality (VR) display and then asked them to walk paths that included several turns and straight segments while we recorded EEG signals. At various intervals, participants were also asked to point in the direction in which a landmark they had previously seen might be (see Fig. 1). These physical navigation tasks required the participants to track their location and orientation through motor efferences and self-motion cues from their visual, vestibular, proprioceptive, and kinesthetic systems. Hence, the data we gathered allowed us to assess the network segregation and integration in the RSC and frontal regions of each walking segment during actual navigation. The results showed that the segregation of the RSC region increased with a higher number of turning points (NT) during physical navigation, reflecting that the navigation load modulated RSC segregation.

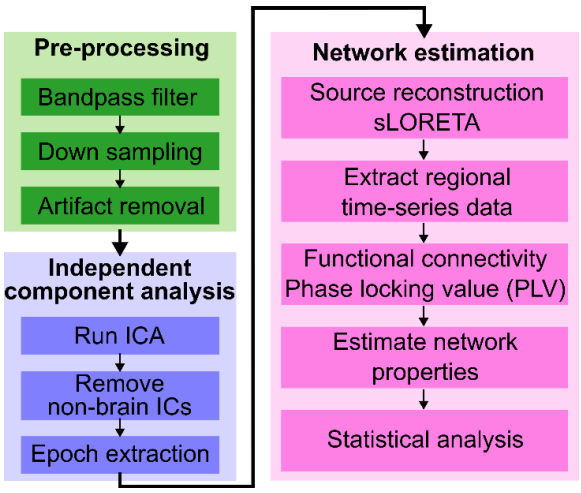

Fig. 2. The pipeline for brain network segregation and integration analysis.

II. Materials and Methods

A. Participants

Eighteen healthy adults (age 27.8 ± 4.2 years, two females) participated in this experiment. All participants reported normal or corrected-to-normal vision. The participants were first provided instructions about the experiment and then signed the consent form if they agreed to perform the experiment. Each participant received $60 for participating in the experiment. The protocol was approved by the University of Technology Sydney (UTS).

B. Data recording

The scenario was developed under Unity (version 2017.3) with the VRTK plugin. The experiment was performed in the VR environment using a head-mounted display (HTC Vive Pro; 2x 1440 x 1600 resolution, 90 Hz refresh rate, 110° field of view) with binocular eye-tracking (Pupil-lab, Berlin, Germany). All the data streams from the EEG and VR events were synchronized by the Lab Streaming Layer [28]. EEG data were recorded from 64 active-wet electrodes with a sampling rate of 500 Hz (LiveAmps System, Brain Products, Gilching, Germany). Electrodes were placed on an elastic cap with an equidistant design (EASYCAP, Herrsching, Germany). Data were referenced to an electrode located closest to the standard position FCz. The impedance of all sensors was kept below 5 kΩ.

C. Experimental design

Participants first observed a global landmark that they had to remember. Then, the landmark disappeared, and participants navigated along a predefined path, including several turns to the left or right. The path comprised a straight segment and turns. A virtual red sphere floating at eye height indicated the endpoint of each straight segment. Participants had to walk toward the red sphere, which disappeared upon collision. At the end of the first walk, after two or three turns, participants performed a spatial-retrieval task, a letter-encoding task, and a letter-retrieval task. Subsequently, participants walked and finished the second walk, including two or three turns, which was similar to the first walk. At the end of the second walk, participants performed the spatial-retrieval and letter-retrieval tasks.

At the beginning of the trial, the participant had 4 seconds to remember the landmark position before the landmark disappeared. Next, the participant responded to the question “where is the landmark location?” by pointing the controller to the expected landmark location and clicking the hair trigger of a controller (Resp. 1, Fig. 1). After the first response, the participant heard a beep sound indicating that they should start navigating. During the first walk, the red sphere disappeared once the participant reached the sphere position. S/he, then, needed to find another red sphere and navigate toward it (walk 1x, 1 indicating the first walk, and x indicating the number of the red sphere, Fig. 1) while keeping track of their spatial location. When participants reached the last red sphere, the text message “Attention” appeared in front of them and lasted for a 3 second period, and the participant stopped walking and prepared for the next spatial-retrieval task.

In this spatial-retrieval task, the participant answered the question “where is the landmark location?” by pointing the controller to the remembered landmark location and clicking the hair trigger of the controller (Resp. 2, Fig. 1). After that, they answered the question “where is the starting location?” by pointing the controller to select one out of two homing arrows that were presented in front of them pointing to the left or the right.

Next, the participant performed the letter-encoding task with three distinctive levels of three, five, or seven letters out of the 26 letters of the English alphabet in random order. The purpose of this letter-encoding task was to increase the cognitive mental workload of the participants. The time interval between letters was 1 second. Then, the participant answered the question of whether a letter belonged to the letter list by clicking the hair trigger (yes) or touchpad (no) (Resp. 3, Fig. 1).

After Resp. 3, participants had 2 seconds of rest before starting the second walk (the second navigation phase) cued by the beep sound; in the second walk, participants were to walk toward the red sphere (walk 2x, Fig. 1) while memorizing the set of letters and the landmark location. Once the second walk was finished, the participant answered the question of whether a letter belonged to the letter list (Resp. 4, Fig. 1). Then, the participant answered the questions, “where is the landmark location?” and “where is the starting location?” (Resp. 5, Fig. 1). After that, the participants finished the trial and started the next trial once they clicked both grip bottoms on the controller based on their readiness.

Participants performed four learning trials first to familiarize themselves with the experiment tasks after receiving instructions from the experimenter. Participants then started the main experiment once they were ready. The main experiment consisted of 3 sessions of 30 trials each. Participants had a rest period of 5-10 minutes between sessions and 3-10 seconds between trials based on their readiness.

D. EEG analysis

All the preprocessing steps were performed in EEGLAB (version 14.2.0) [29, 30] (and adapted from Do, et al. [31]) . The EEG data were first bandpass filtered (1-100 Hz) and then downsampled to 250 Hz. Next, all idle segments with zero values in the raw data (continuous data) were removed (threshold=3 seconds). Then, the bad channels were identified and removed based on the correlations with other channels (threshold=0.85) and the abnormal data distributions (standard deviation=4), and the missing channels were interpolated by applying the sphere method. Next, the noisy portions of the continuous data were removed through automatic continuous data cleaning based on the spectrum value (threshold=10 dB) and power, with a criteria of maximum bad channels (maximum fraction of bad channels=0.15) and relative to a robust estimate of the clean EEG power distribution in the channel ([minimum, maximum]=[-3.5 5]). Next, all the EEG channel data was re-referenced to the average. Subsequently, adaptive mixed independence component analysis (AMICA) was applied to the re-referenced data to decompose them into maximally independent components (ICs). Then, the dipole-fitting routine [32] was applied to identify the locations of the ICs. Next, the AMICA solution was copied back to the re-referenced dataset. The nonbrain components were identified and removed by using the IClabel toolbox [33] (with a confident threshold > 95%) before extracting data from six walking navigation segments with respect to the NT during navigation. Then, the bad epochs were identified and removed by checking the raw value (threshold = 100 μV).

E. Functional connectivity

The data from a trial was epoched into various walking segments with respect to the turning point sequence. Then, the participant data per walking condition was calculated by averaging the walking segment conditions. Finally, the participant data for the six walking conditions were used for the group analysis.

First, the distributed source localization was used to address the inverse problem. The dipole brain source localization activity was estimated from cleaned epoched data, and then the brain FC was estimated from the source activity by using the Brainstorm toolbox (version 02-Jun-2020) [34]. The epoched data were first coregistered with the MRI template ("ICBM152" template [35]) and EEG sensor locations (same template for all participants) in the same anatomical landmarks. Next, the lead field of the cortical mesh (15,002 vertices, 29984 faces) was estimated by using openMEEG [36, 37]. The noise covariance matrix was calculated using the idle period during the experiment. An atlas-based segmentation approach was used to project the EEG data onto an anatomical framework consisting of 68 cortical regions identified by means of re-segmenting the Desikan-Killiany [38] atlas using FreeSurfer [39]. Then, a standardized low-resolution brain electromagnetic tomography (sLORETA) method [40] was used to reconstruct the regional time series from the 68 brain regions. Finally, the FC among regions was estimated by the phase-locking value (PLV) (eq. 1) [41] in four various frequency bands: delta (1–4 Hz), theta (4–8 Hz), alpha (8–12 Hz), and beta (12–30 Hz). Then, the highest 10% (of the highest PLV values) were kept for further estimating the network properties [42], and the remaining PLV values were set to zero.

Phase-locking value:

$$PLV(t) = \left|\frac{1}{\delta}\int_{t-\delta/2}^{t+\delta/2} e^{j(\varphi_y(t)-\varphi_x(t))}d\tau\right| \quad (1)$$

where $\varphi_y(t)$ and $\varphi_x(t)$ indicate the phases of the time series signals x and y at time t, respectively, and δ indicates the size of the window. PLV values ranged between 0 (no phase-locking) and 1 (full synchrony).

F. Network properties

The network properties (segregation and integration) were calculated from the PLV connectivity matrix at each frequency of each walking segment. The network segregation indicated the local information processing at each node (each cortical region) related to the experimental task, while network integration indicated the global information exchanged at each node (each cortical region) related to the experimental task. The network properties were calculated for all walking segments of each participant. Then, a statistical test was conducted to check the impact of the walking sequence on the network properties. In this study, we used the clustering coefficient (eq. 2), which reflected local information processing in each region [43, 44], to measure segregation and the participation coefficient (eq. 3), which reflected global information processing in each region [45], to measure integration. Both measurements were calculated using the Brain Connectivity Toolbox [46].

Network segregation:

$$C_i = \frac{2t_i}{k_i(k_i-1)'} \quad (2)$$

where t_i represents the number of triangles around node i and k_i indicates the number of edges connected to node i. The clustering coefficient is the portion of links among a node's neighbors divided by the number of connections that could exist between them, which is 0 if no connections exist and 1 if all neighbors are connected.

Network integration:

$$P_i = 1 - \sum_{s=1}^{N_m}\left(\frac{k_{is}}{k_i}\right)^2 \quad (3)$$

where N_m indicates the number of modules, k_{is} represents the number of edges between node i and the other nodes in module s, and k_i is the total degree of node i. The participation coefficient of a node is close to 0 if all of its links are within its own module and 1 if its links are uniformly distributed among all the modules.

III. Results

A. Behavioral performance

The absolute value of the angular difference between the participant to the landmark vector and the participant's pointing vector was measured as the landmark-pointing error. Linear regression was conducted to determine whether the NT affected participants' pointing errors. The landmark-pointing error (in degrees) was significantly different under different NTs using the Friedman test, $\chi2(5)=53.34$, $p<0.0001$. A significant regression equation was found ($F(5,96)=9.18$, $p<0.0001$), with an R^2 of 0.32. Then, the Wilcoxon sign-rank test was used to check the significant difference in participants' pointing landmark errors between various NTs (Table 1).

B. Functional connectivity

The group average FC was estimated across six walking segments (Fig. 4, visualized by the BrainNet Viewer [47]). Then, the Friedman test was recruited to measure the significant differences in the network properties (segregation was measured by the clustering coefficient, and integration was measured by the participation coefficient) across walking segments, followed by the post hoc pairwise Wilcoxon signed-rank test (FDR-corrected). For network segregation, the Friedman test showed significant differences in the frontal delta band ($\chi2(5)=23.18$, $p=0.00031$), frontal theta band ($\chi2(5)=12.93$, $p=0.024$), frontal alpha band ($\chi2(5)=14.61$, $p=0.012$), and RSC theta band ($\chi2(5)=17.44$, $p=0.0037$). For network integration, the Friedman test showed significant differences in the frontal theta band ($\chi2(5)=18.68$, $p=0.0022$). Post hoc pairwise Wilcoxon signed-rank (FDR-corrected) results showed that there was a significant difference in the clustering coefficient in the frontal theta (segment 1 and segment 5, $p=0.042$; segment 2 and segment 5, $p=0.042$); frontal alpha (segment 1 and segment 4, $p=0.049$; segment 1 and segment 6, $p=0.025$; segment 3 and segment 4, $p=0.027$; segment 3 and segment 6, $p=0.025$), and RSC theta (segment 2 and segment 6, $p=0.011$; segment 3 and segment 6, $p=0.018$; segment 4 and segment 6, $p=0.007$; segment 5 and segment 6, $p=0.046$) values.

TABLE 1
ERRORS IN THE LANDMARK-POINTING TASK

Number of turning points (NT)		p-adjust value
0	2	0.000046^{****}
0	3	0.000046^{****}
0	4	0.000046^{****}
0	5	0.000046^{****}
0	6	0.000046^{****}
2	3	1.0
2	4	0.007^{**}
2	5	0.1
2	6	0.075
3	4	0.000114^{***}
3	5	0.1
3	6	0.003^{**}
4	5	0.1
4	6	0.876
5	6	0.114

The first and second columns indicate the numbers of turning points, and the third column contains the *p*-values (FDR-adjusted) calculated using the Wilcoxon signed-rank tests (*, **, ***, and **** indicate p<.05, p<.01, p<.001, and p<.0001, respectively).

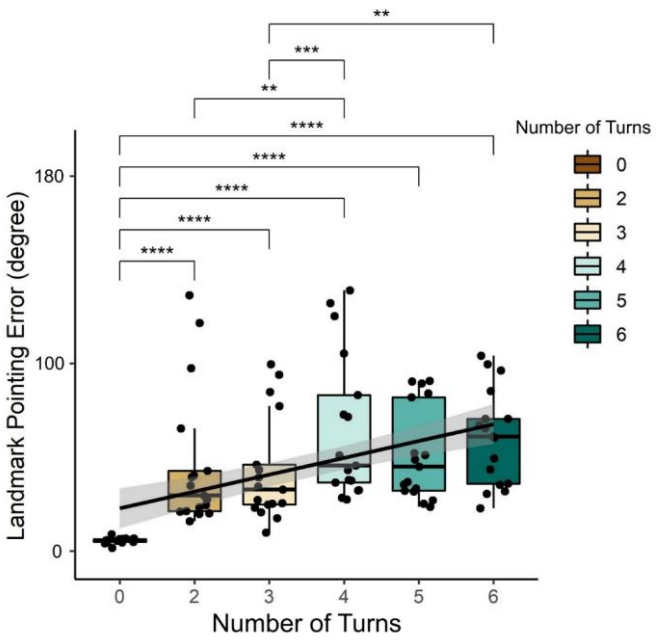

Fig. 3. The landmark-pointing response error (absolute) across walking segments with a distinct NT during the navigation trial. The Wilcoxon signed-rank tests were used to check for significant differences between behavior performance (*, **, ***, and **** indicate p<0.05, p<0.01, p<0.001, and p<0.0001, respectively).

IV. Discussion

Spatial navigation is a vital aspect of many daily activities that require updating position and orientation information as well as computing a homing trajectory. The present study addressed these processes in an active navigation task under various mental workload conditions by manipulating the NT that allowed navigators to move through a large virtual space. We recorded and analyzed the brain activities of navigating participants using the MoBI approach [25-27, 48, 49]. We found that participant performance measured by landmark-pointing errors increased as the navigation load increased, which was manipulated by the NT during navigation. In addition, we found that this navigation load covaried with RSC segregation. When the NT increased, RSC segregation increased in the theta band measured by the PLV connectivity matrix.

First, we analyzed participants' behavior in the landmark

point task to check the effect of turning points on navigation performance. As expected, landmark-pointing errors increased as the NT increased (Fig. 3). In other words, the behavioral results revealed that an increasing NT led to greater difficulty in navigation. Therefore, the NT in this experimental design manipulated the navigation load. The possible explanation for this decline in path integration performance could be bias from the velocity estimation [50] or leaky integration [51]. However, in the present study, participants actively ambulated from a location to several other locations; thus, the brain can receive rich information from the motor efference, visual, proprioceptive, vestibular, and kinesthetic systems. Therefore, the main corruption factor for this decline in landmark-pointing performance could be explained by the Stangl, et al. [52] model. The accumulating noise in the traveled distance increased with the NT, which led to increased error in the pointing task.

Spatial navigation involves several brain regions that communicate and exchange information via the brain network. The synchronization of cortical oscillations has been believed to be a mechanism for this communication and computation [53]. Through a specific frequency, a subpopulation of the neuronal population will likely be coactivated, interact with other regions, and exchange information. Therefore, the synchronization among brain regions reflects both the segregation of the cortical population for processing incoming information and integration among regions for transferring information [54]. Thus, we further investigated the brain dynamics in each walking segment under specific frequencies, which may reflect processing during active navigation. There is a growing body of evidence demonstrating that theta-band oscillation plays a role in memory encoding [23], retrieval [55], and grid-cell generating [9, 10] The theta phase has been reported as a plausible mechanism for neuronal computation and communication [54]. In addition, theta oscillation was reported as an important mechanism for head direction (HD) cell activities [22]. Therefore, investigating the brain network properties that were analyzed in the theta band might reflect the underlying mechanism of the brain regions subserving cognitive navigation processing. The results of the network segregation further showed that navigation pointing errors seems to correspond to frontal segregation (Fig. 5a). A higher

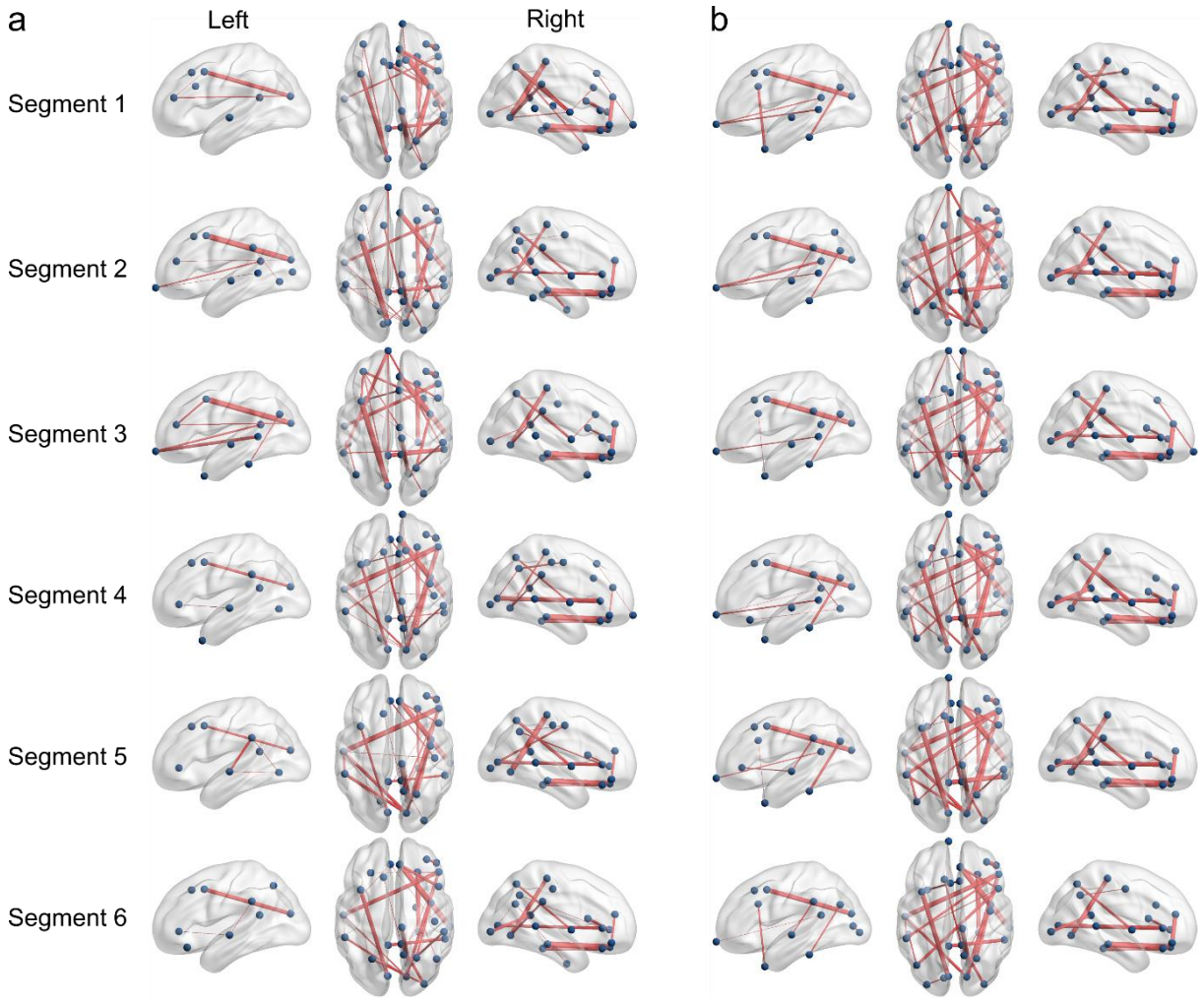

Fig. 4. Functional connectivity of the brain network across six walking segments in the (a) theta band and (b) alpha band. The nodes indicate brain regions (based on 68 Desikan-Killiany atlas). The edges indicate a significant connection between nodes; the edge size indicates the strength of the connection.

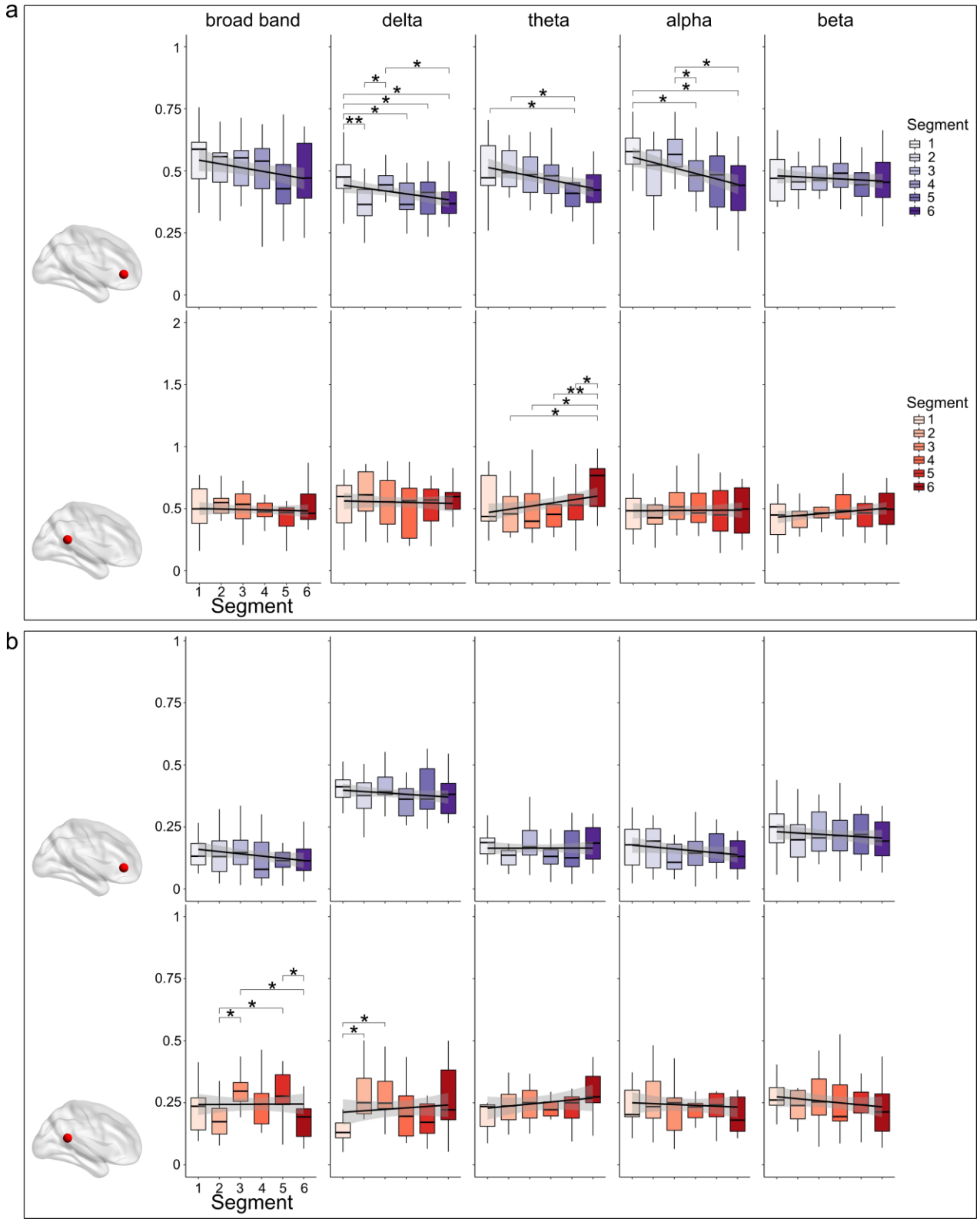

Fig. 5. Graph properties at the frontal and retrosplenial complex (RSC): (a) Clustering coefficient (a) and (b) participation coefficient across six walking segments in various frequency ranges. Pairwise post hoc Wilcoxon signed-rank tests (FDR-corrected) were used to check for significant differences between walking segments (* and ** indicate $p<0.05$ and $p<0.01$, respectively).

NT led to poorer behavioral performance and a decrease in frontal segregation in the theta band.

Remarkably, in the present work, we found that RSC segregation increased with an increased NT at the theta band (Fig. 5a). This result revealed that RSC activity was modulated by the navigation load (NT). The RSC coordinates with the parietal and occipital regions to translate different spatial reference frames [8]. In addition, the RSC

communicates with the hippocampus to update the spatial information of the cognitive map, which is in the form of an allocentric framework [8, 56]. Furthermore, HD cells are present in several regions in the brain, including the RSC [5]. HD cells exchange information across the network via theta oscillation to modulate grid cell formation in the parahippocampus [22]. As a result, considering the brain as a complex system, the RSC plays a role as a hub in the brain network to coordinate the in and out spatial information. In previous studies [6, 7], the experimental setup was performed in the stationary condition with only an optical flow visual information stimulus, and the head direction activity, which obtains input from the vestibular system, might be attenuated. In the current study, participants could freely navigate and receive richer sensory information via their movements. Thus, the activity of the RSC might depend on the amount of spatial information that needed to be processed. Therefore, when the navigation load increased, the local information processed in the RSC was higher, which was measured by the clustering coefficient. These study results provide the first evidence that RSC activity covaries with spatial information processing.

V. Conclusion

Altogether, this study explored the behavioral and neural dynamics in active spatial navigation under various workload conditions. The behavior showed increased errors in the landmark-pointing task when the NT increased. We further investigated neural activity to determine the underlying mechanism of this phenomenon. We found that the local information processing via the RSC increased when the NT increased, reflecting that the RSC plays an important role in coordinating and processing information in active navigation. In addition, we also found that the decline in frontal segregation was associated with spatial navigation performance. These findings demonstrate that brain dynamics systematically vary in stationary and physical navigation experiments. The change in RSC segregation could be an important feature for monitoring navigation workload when actively exploring a space.

References

[1] C. F. Doeller, C. Barry, and N. Burgess, "Evidence for grid cells in a human memory network," *Nature,* vol. 463, no. 7281, pp. 657-661, 2010.

[2] A. D. Ekstrom, M. J. Kahana, J. B. Caplan, T. A. Fields, E. A. Isham, E. L. Newman, and I. Fried, "Cellular networks underlying human spatial navigation," *Nature,* vol. 425, no. 6954, pp. 184, 2003.

[3] B. L. McNaughton, F. P. Battaglia, O. Jensen, E. I. Moser, and M.-B. Moser, "Path integration and the neural basis of the'cognitive map'," *Nature Reviews Neuroscience,* vol. 7, no. 8, pp. 663, 2006.

[4] K. E. Cullen, and J. S. Taube, "Our sense of direction: progress, controversies and challenges," *Nature neuroscience,* vol. 20, no. 11, pp. 1465, 2017.

[5] R. A. Epstein, "Parahippocampal and retrosplenial contributions to human spatial navigation," *Trends in cognitive sciences,* vol. 12, no. 10, pp. 388-396, 2008.

[6] K. Gramann, J. Onton, D. Riccobon, H. J. Mueller, S. Bardins, and S. Makeig, "Human brain dynamics accompanying use of egocentric and allocentric reference frames during navigation," *Journal of cognitive neuroscience,* vol. 22, no. 12, pp. 2836-2849, 2010.

[7] C.-T. Lin, T.-C. Chiu, and K. Gramann, "EEG correlates of spatial orientation in the human retrosplenial complex," *NeuroImage,* vol. 120, pp. 123-132, 2015.

[8] S. D. Vann, J. P. Aggleton, and E. A. Maguire, "What does the retrosplenial cortex do?," *Nature Reviews Neuroscience,* vol. 10, no. 11, pp. 792-802, 2009.

[9] V. D. Bohbot, M. S. Copara, J. Gotman, and A. D. Ekstrom, "Low-frequency theta oscillations in the human hippocampus during real-world and virtual navigation," *Nature Communications,* vol. 8, pp. 14415, 2017.

[10] Z. M. Aghajan, P. Schuette, T. A. Fields, M. E. Tran, S. M. Siddiqui, N. R. Hasulak, T. K. Tcheng, D. Eliashiv, E. A. Mankin, and J. Stern, "Theta oscillations in the human medial temporal lobe during real-world ambulatory movement," *Current Biology,* vol. 27, no. 24, pp. 3743-3751. e3, 2017.

[11] J. M. Shine, "Neuromodulatory influences on integration and segregation in the brain," *Trends in cognitive sciences,* 2019.

[12] M. Y. Chan, D. C. Park, N. K. Savalia, S. E. Petersen, and G. S. Wig, "Decreased segregation of brain systems across the healthy adult lifespan," *Proceedings of the National Academy of Sciences,* vol. 111, no. 46, pp. E4997-E5006, 2014.

[13] B. King, P. Van Ruitenbeek, I. Leunissen, K. Cuypers, K.-F. Heise, T. Santos Monteiro, L. Hermans, O. Levin, G. Albouy, and D. Mantini, "Age-related declines in motor performance are associated with decreased segregation of large-scale resting state brain networks," *Cerebral Cortex,* vol. 28, no. 12, pp. 4390-4402, 2018.

[14] K. Cassady, H. Gagnon, P. Lalwani, M. Simmonite, B. Foerster, D. Park, S. J. Peltier, M. Petrou, S. F. Taylor, and D. H. Weissman, "Sensorimotor network segregation declines with age and is linked to GABA and to sensorimotor performance," *Neuroimage,* vol. 186, pp. 234-244, 2019.

[15] K. K. Ng, J. C. Lo, J. K. Lim, M. W. Chee, and J. Zhou, "Reduced functional segregation between the default mode network and the executive control network in healthy older adults: a longitudinal study," *Neuroimage,* vol. 133, pp. 321-330, 2016.

[16] J. R. Cohen, and M. D'Esposito, "The segregation and integration of distinct brain networks and their relationship to cognition," *Journal of Neuroscience,* vol. 36, no. 48, pp. 12083-12094, 2016.

[17] J. M. Shine, P. G. Bissett, P. T. Bell, O. Koyejo, J. H. Balsters, K. J. Gorgolewski, C. A. Moodie, and R. A. Poldrack, "The dynamics of functional brain networks: Integrated network states during cognitive task performance," *Neuron,* vol. 92, no. 2, pp. 544-554, 2016.

[18] P. Fransson, B. C. Schiffler, and W. H. Thompson, "Brain network segregation and integration during an epoch-related working memory fMRI experiment," *Neuroimage,* vol. 178, pp. 147-161, 2018.

[19] D. S. Bassett, M. Yang, N. F. Wymbs, and S. T. Grafton, "Learning-induced autonomy of sensorimotor systems," *Nature neuroscience,* vol. 18, no. 5, pp. 744-751, 2015.

[20] M. P. Brandon, A. R. Bogaard, C. P. Libby, M. A. Connerney, K. Gupta, and M. E. Hasselmo, "Reduction of theta rhythm dissociates grid cell spatial periodicity from directional tuning," *Science,* vol. 332, no. 6029, pp. 595-599, 2011.

[21] J. Koenig, A. N. Linder, J. K. Leutgeb, and S. Leutgeb, "The spatial periodicity of grid cells is not sustained during reduced theta oscillations," *Science,* vol. 332, no. 6029, pp. 592-595, 2011.

[22] S. S. Winter, B. J. Clark, and J. S. Taube, "Disruption of the head direction cell network impairs the parahippocampal grid cell signal," *Science,* vol. 347, no. 6224, pp. 870-874, 2015.

[23] J. Onton, A. Delorme, and S. Makeig, "Frontal midline EEG dynamics during working memory," *Neuroimage,* vol. 27, no. 2, pp. 341-356, 2005.

[24] A. Mohan, D. De Ridder, and S. Vanneste, "Graph theoretical analysis of brain connectivity in phantom sound perception," *Scientific reports,* vol. 6, 2016.

[25] S. Makeig, K. Gramann, T.-P. Jung, T. J. Sejnowski, and H. Poizner, "Linking brain, mind and behavior," *International Journal of Psychophysiology,* vol. 73, no. 2, pp. 95-100, 2009.

[26] K. Gramann, J. T. Gwin, D. P. Ferris, K. Oie, T.-P. Jung, C.-T. Lin, L.-D. Liao, and S. Makeig, "Cognition in action: imaging

brain/body dynamics in mobile humans," *Reviews in the Neurosciences,* vol. 22, no. 6, pp. 593-608, 2011.

[27] K. Gramann, T.-P. Jung, D. P. Ferris, C.-T. Lin, and S. Makeig, "Toward a new cognitive neuroscience: modeling natural brain dynamics," *Frontiers in human neuroscience,* vol. 8, 2014.

[28] C. Kothe, "Lab streaming layer (LSL)," Accessed on October 26, 2015 (2014).

[29] A. Delorme, and S. Makeig, "EEGLAB: an open source toolbox for analysis of single-trial EEG dynamics including independent component analysis," *Journal of neuroscience methods,* vol. 134, no. 1, pp. 9-21, 2004.

[30] A. Delorme, T. Mullen, C. Kothe, Z. A. Acar, N. Bigdely-Shamlo, A. Vankov, and S. Makeig, "EEGLAB, SIFT, NFT, BCILAB, and ERICA: new tools for advanced EEG processing," *Computational intelligence and neuroscience,* vol. 2011, pp. 10, 2011.

[31] T.-T. N. Do, C.-T. Lin, and K. Gramann, "Human retrosplenial theta and alpha modulation in active spatial navigation," *bioRxiv,* pp. 406124, 2020.

[32] R. Oostenveld, and T. F. Oostendorp, "Validating the boundary element method for forward and inverse EEG computations in the presence of a hole in the skull," *Human brain mapping,* vol. 17, no. 3, pp. 179-192, 2002.

[33] L. Pion-Tonachini, K. Kreutz-Delgado, and S. Makeig, "ICLabel: An automated electroencephalographic independent component classifier, dataset, and website," *NeuroImage,* vol. 198, pp. 181-197, 2019.

[34] F. Tadel, S. Baillet, J. C. Mosher, D. Pantazis, and R. M. Leahy, "Brainstorm: a user-friendly application for MEG/EEG analysis," *Computational intelligence and neuroscience,* vol. 2011, 2011.

[35] V. S. Fonov, A. C. Evans, R. C. McKinstry, C. Almli, and D. Collins, "Unbiased nonlinear average age-appropriate brain templates from birth to adulthood," *NeuroImage,* no. 47, pp. S102, 2009.

[36] A. Gramfort, T. Papadopoulo, E. Olivi, and M. Clerc, "OpenMEEG: opensource software for quasistatic bioelectromagnetics," *Biomedical engineering online,* vol. 9, no. 1, pp. 45, 2010.

[37] J. Kybic, M. Clerc, T. Abboud, O. Faugeras, R. Keriven, and T. Papadopoulo, "A common formalism for the integral formulations of the forward EEG problem," *IEEE transactions on medical imaging,* vol. 24, no. 1, pp. 12-28, 2005.

[38] R. S. Desikan, F. Ségonne, B. Fischl, B. T. Quinn, B. C. Dickerson, D. Blacker, R. L. Buckner, A. M. Dale, R. P. Maguire, and B. T. Hyman, "An automated labeling system for subdividing the human cerebral cortex on MRI scans into gyral based regions of interest," *Neuroimage,* vol. 31, no. 3, pp. 968-980, 2006.

[39] B. Fischl, "FreeSurfer," *Neuroimage,* vol. 62, no. 2, pp. 774-781, 2012.

[40] R. D. Pascual-Marqui, "Standardized low-resolution brain electromagnetic tomography (sLORETA): technical details," *Methods Find Exp Clin Pharmacol,* vol. 24, no. Suppl D, pp. 5-12, 2002.

[41] J. P. Lachaux, E. Rodriguez, J. Martinerie, and F. J. Varela, "Measuring phase synchrony in brain signals," *Human brain mapping,* vol. 8, no. 4, pp. 194-208, 1999.

[42] J. Rizkallah, J. Annen, J. Modolo, O. Gosseries, P. Benquet, S. Mortaheb, H. Amoud, H. Cassol, A. Mheich, and A. Thibaut, "Decreased integration of EEG source-space networks in disorders of consciousness," *NeuroImage: Clinical,* vol. 23, pp. 101841, 2019.

[43] D. J. Watts, and S. H. Strogatz, "Collective dynamics of 'small-world'networks," *Nature,* vol. 393, no. 6684, pp. 440-442, 1998.

[44] E. Bullmore, and O. Sporns, "Complex brain networks: graph theoretical analysis of structural and functional systems," *Nature Reviews Neuroscience,* vol. 10, no. 3, pp. 186-198, 2009.

[45] R. Guimera, and L. A. N. Amaral, "Functional cartography of complex metabolic networks," *Nature,* vol. 433, no. 7028, pp. 895-900, 2005.

[46] M. Rubinov, and O. Sporns, "Complex network measures of brain connectivity: uses and interpretations," *Neuroimage,* vol. 52, no. 3, pp. 1059-1069, 2010.

[47] M. Xia, J. Wang, and Y. He, "BrainNet Viewer: a network visualization tool for human brain connectomics," *PloS one,* vol. 8, no. 7, 2013.

[48] E. Jungnickel, L. Gehrke, M. Klug, and K. Gramann, "MoBI—Mobile Brain/Body Imaging," *Neuroergonomics,* pp. 59-63: Elsevier, 2019.

[49] C.-T. Lin, and T.-T. N. Do, "Direct-Sense Brain-Computer Interfaces and Wearable Computers," *IEEE Transactions on Systems, Man, and Cybernetics: Systems,* vol. 51, no. 1, pp. 298-312, 2021.

[50] K. J. Lakshminarasimhan, M. Petsalis, H. Park, G. C. DeAngelis, X. Pitkow, and D. E. Angelaki, "A dynamic Bayesian observer model reveals origins of bias in visual path integration," *Neuron,* vol. 99, no. 1, pp. 194-206. e5, 2018.

[51] M. Lappe, M. Jenkin, and L. R. Harris, "Travel distance estimation from visual motion by leaky path integration," *Experimental brain research,* vol. 180, no. 1, pp. 35-48, 2007.

[52] M. Stangl, I. Kanitscheider, M. Riemer, I. Fiete, and T. Wolbers, "Sources of path integration error in young and aging humans," *Nature communications,* vol. 11, no. 1, pp. 1-15, 2020.

[53] Z. Nadasdy, "Binding by asynchrony: the neuronal phase code," *Frontiers in Neuroscience,* vol. 4, pp. 51, 2010.

[54] J. F. Cavanagh, and M. J. Frank, "Frontal theta as a mechanism for cognitive control," *Trends in cognitive sciences,* vol. 18, no. 8, pp. 414-421, 2014.

[55] D. J. Mitchell, N. McNaughton, D. Flanagan, and I. J. Kirk, "Frontal-midline theta from the perspective of hippocampal "theta"," *Progress in neurobiology,* vol. 86, no. 3, pp. 156-185, 2008.

[56] R. A. Epstein, E. Z. Patai, J. B. Julian, and H. J. Spiers, "The cognitive map in humans: spatial navigation and beyond," *Nature neuroscience,* vol. 20, no. 11, pp. nn. 4656, 2017.

SUPPLEMENTARY

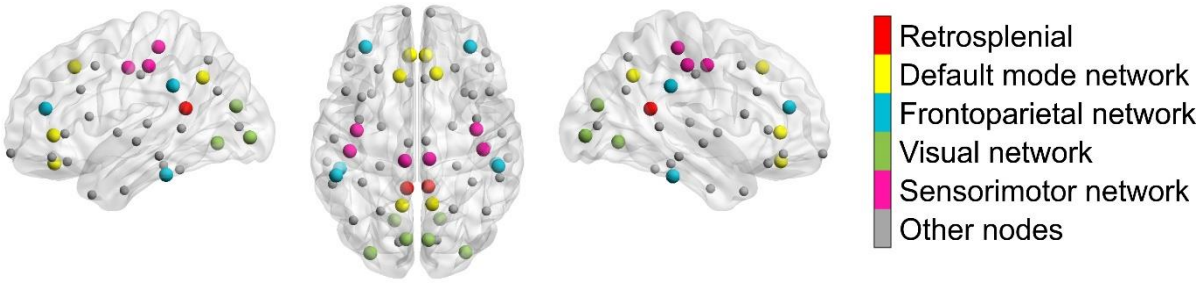

Fig. S1. Network atlas.

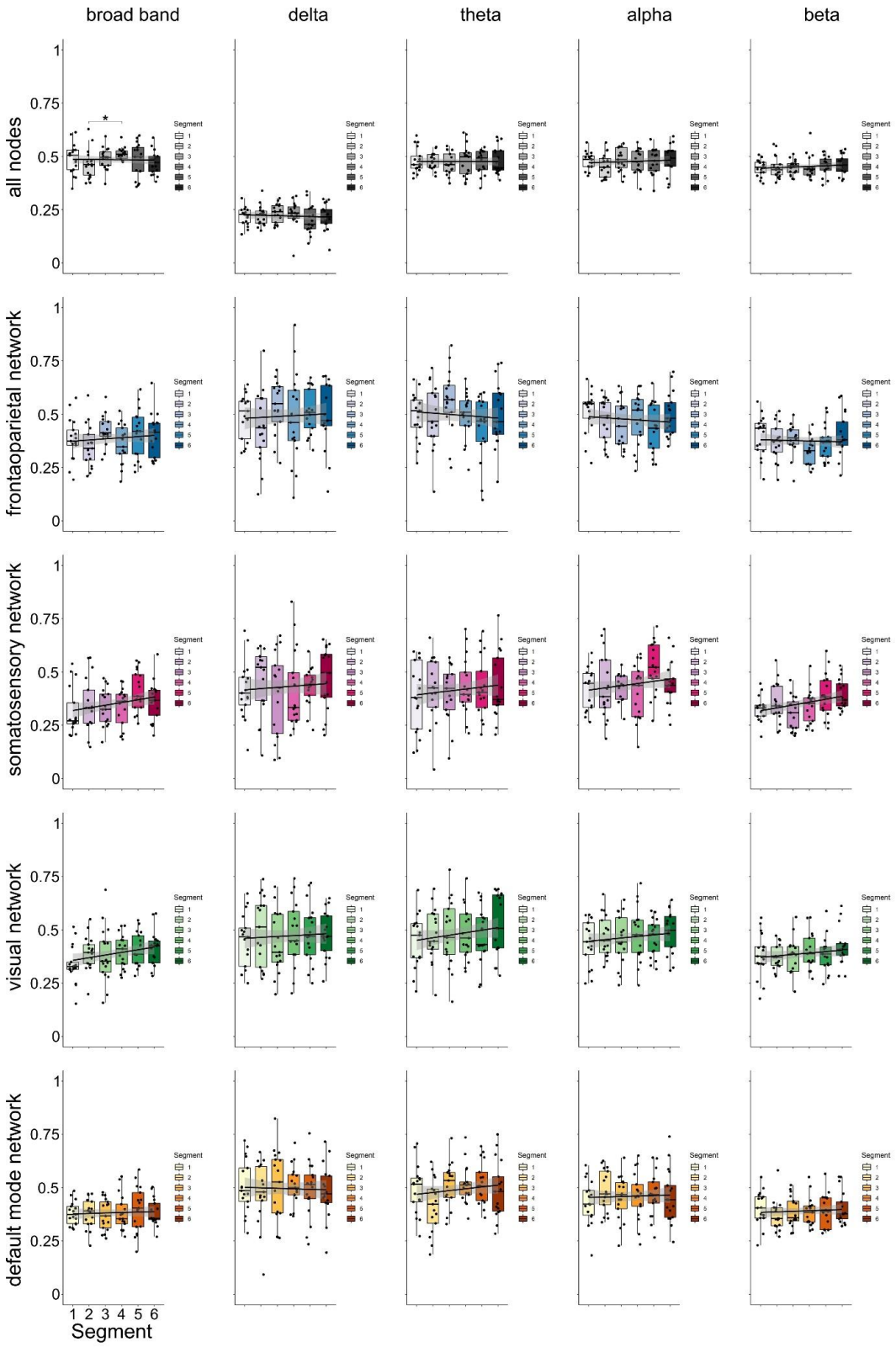

Fig. S2. Clustering coefficient among various brain networks, including the whole-brain network, frontoparietal network, somatosensory network, visual network, and default mode network, across walking segments under various frequencies.

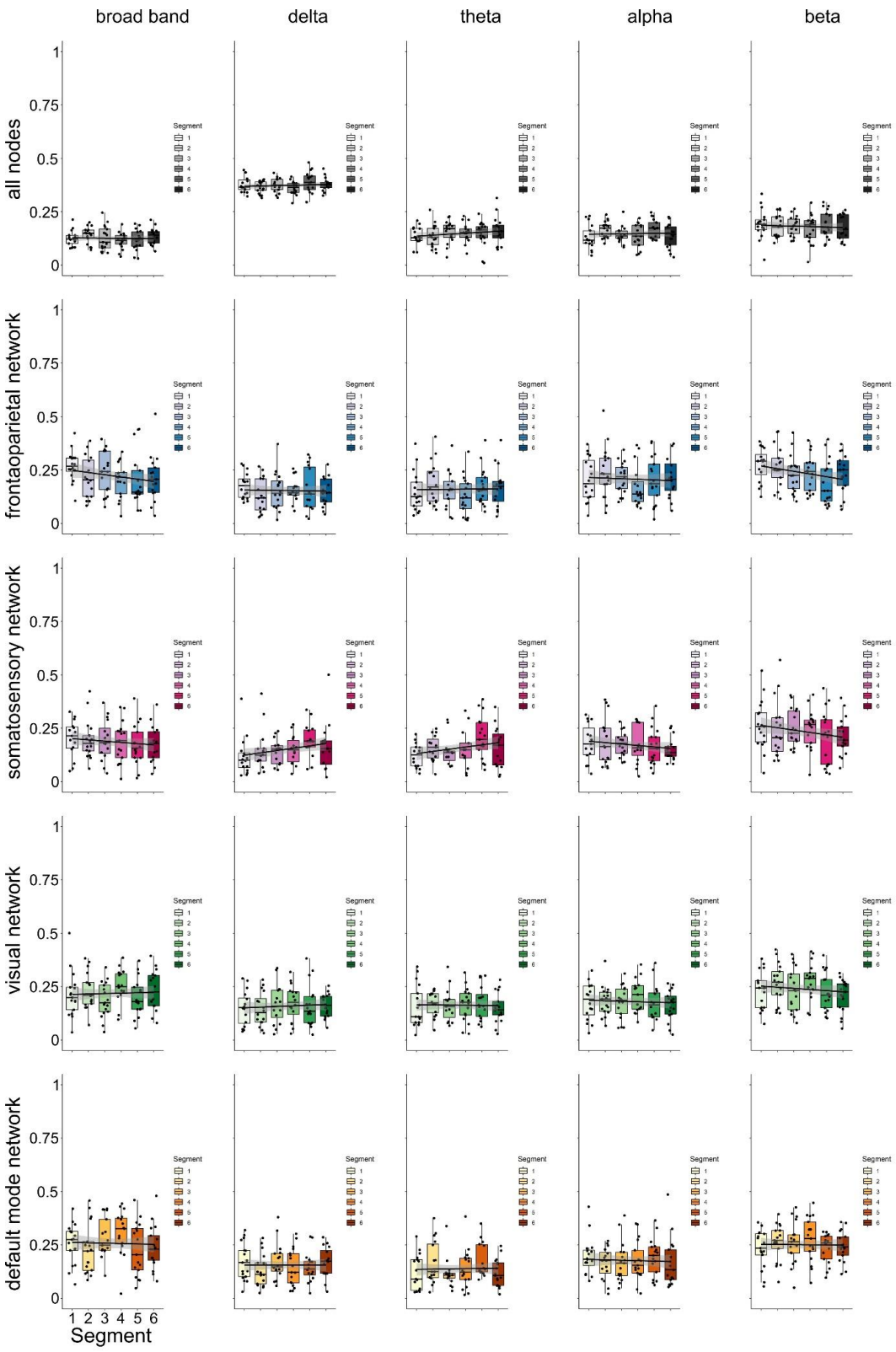

Fig. S3. Participation coefficients among various brain networks, including the whole-brain network, frontoparietal network, somatosensory network, visual network, and default mode network, across walking segments under various frequencies.